Available online at www.sciencedirect.com

SciVerse ScienceDirect

Ceramics International 39 (2013) 4765–4769

CERAMICS INTERNATIONAL

www.elsevier.com/locate/ceramint

Effects of Cr content and morphology on the luminescence properties of the Cr-doped alpha-Al_2O_3 powders

Dianguang Liu*

National Key Laboratory of Thermostructure Composite, Northwestern Polytechnical University, Xi'an, Shaanxi 710072, China

Received 18 October 2012; accepted 22 November 2012
Available online 29 November 2012

Abstract

Al_2O_3:Cr^{3+} samples were synthesized via hydrothermal and microwave solvothermal methods and thermal decomposition of Cr^{3+} doped precursors. The sample characterizations were carried out by means of X-ray diffraction (XRD), scanning electron microscope (SEM), photoluminescence (PL) spectra and decay curves. XRD results indicated that Cr^{3+} doped samples were pure α-Al_2O_3 phase after being calcined at 1573 K. SEM results showed that the length and diameter of these Cr^{3+} doped alumina microfibers by hydrothermal route were about 2–5 μm and 100–300 nm, respectively; the obtained α-Al_2O_3 based powders via the microwave solvothermal method were microspheres with an average diameter about 1–2 μm. PL spectra showed that the Al_2O_3:Cr^{3+} samples presented a broad R band at 696 nm. It is shown that the 0.3 mol% of doping concentration of Cr^{3+} ions in α-Al_2O_3:Cr^{3+} is optimum. According to Dexter's theory, the critical distance between Cr^{3+} ions for energy transfer was determined to be 24 Å. It is found that the curve followed the single-exponential decay. Furthermore, the luminescence properties of the samples are also dependent on the morphology.

Keywords: C. Optical properties; D. Al_2O_3

1. Introduction

Inorganic luminescence materials have drawn great attention, as they are widely applied in light emitting display, lasers, optoelectronics, and as fluorescent markers in biomedicine [1–4]. As the shape of nanoscale materials has a pronounced influence on their physicochemical properties, it is necessary and important to control morphology of the materials. Therefore, much effort has been devoted to fabricating inorganic luminescent materials with specific morphologies, such as wires, rods, sheets, spheres, and flowers [5–9]. Although many investigations have been carried out to study optical properties of the materials, there are a few investigations on the effect of the morphology in materials [5,6].

Herein, we report the controllable synthesis of α-Al_2O_3:Cr^{3+} materials with various morphologies. The luminescence properties are studied in detail and PL spectra indicate that the Al_2O_3:Cr^{3+} samples present excellent red emission at 696 nm excited at 553 nm. The effects of doped content and morphology on α-Al_2O_3 have been systematically discussed.

2. Experimental

2.1. Synthesis of Al_2O_3:Cr^{3+} powders

The Al_2O_3 matrix doped with Cr^{3+} ion was obtained by the following preparation processes: (a) *Hydrothermal route*—8 g poly-glycol (PEG) (Kermel, 99%) with relative molecular mass $M = 20{,}000$, was dissolved in deionized water to form a clear solution, to which 7.5 g $Al(NO_3)_3 \cdot 9H_2O$, different amounts of $Cr(NO_3)_3 \cdot 9H_2O$ (0.1, 0.3, 0.5, 0.7, 0.9 mol%) were added. After the salts were totally dissolved, 20 g urea was added. The mixed solution was further magnetically stirred for 1 h. Then the final mixture was transferred to three Teflon-lined autoclaves of 40 mL capacity and placed in an oven at 393 K. After 24 h, the autoclave being cooled to room temperature, the precipitation were collected and washed several times with deionized water

*Tel./fax: +86 29 88494620.
E-mail address: dianguang12@gmail.com

0272-8842/$ - see front matter © 2012 Elsevier Ltd and Techna Group S.r.l. All rights reserved.
http://dx.doi.org/10.1016/j.ceramint.2012.11.063

and ethanol to remove the impurities, and then dried at 353 K in a vacuum oven for 24 h. The surfactant was removed by calcination in air at 1573 K for 2 h with heating rate of 2 K/min; (b) *Microwave solvothermal method*—In a typical procedure for preparing Al_2O_3:Cr^{3+}, 9 mmol of $AlCl_3 \cdot 6H_2O$, different amounts of $CrCl_3 \cdot 6H_2O$ (0.1, 0.3, 0.5, 0.7, 0.9 mol%), 4.5 g of cetyltrimethyl ammonium bromide (CTAB), and 10.8 g of NaOH were dissolved in a solvent of 261 mL of deionized water and 9 mL of *n*-butyl alcohol. Then, 25 mL of ethyl acetate was added to the mixture and magnetically stirred for several minutes. The resultant reaction systems were loaded into five 100 mL Teflon autoclaves with 55 mL per container, sealed, microwave-heated to 433 K and maintained at this temperature for 30 min, and then cooled down naturally. The microwave oven used for sample preparation was a microwave solvothermal synthesis system (MDS-8, Sineo, Shanghai, China). The precipitate was collected by centrifugation, washed with deionized water and ethanol three times, respectively, and dried in a vacuum at 353 K for 12 h. Subsequently, the samples were annealed for 2 h at a temperature of 1573 K.

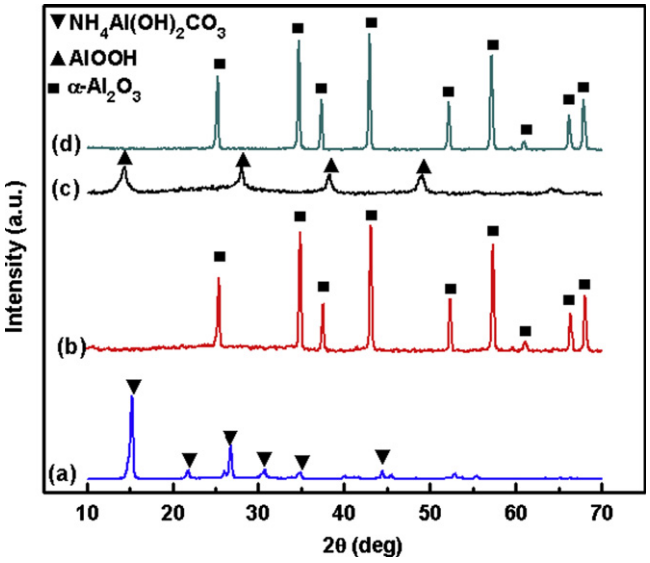

Fig. 1. XRD patterns of the Cr^{3+} doped samples: (a), (c) as-grown from solution and (b), (d) postannealed at 1573 K for 2 h.

2.2. Characterization

The XRD patterns of the samples were recorded on a high resolution X-ray diffractometer (XRD, D/MAX 2200 pc, Japan). Their diffraction patterns were obtained by using Cu Kα radiation of wavelength $\lambda = 0.15418$ nm. The morphology of the powder was recorded by using a field-emission scanning electron microscope (JSM-6700 F, JEOL Japan) operated at 5 kV. The room temperature PL, photoluminescence excitation (PLE) spectra and decay curves of the products were measured by a fluorescence spectrophotometer (Hitachi F-4600) with a 450 W xenon lamp. In all experiments, both excitation and emission slits were 2.5 nm.

3. Results and discussion

3.1. Crystallization behavior and morphology

XRD patterns of the samples, obtained from solution and postannealed at 1573 K, are shown in Fig. 1. As can be seen from Fig. 1 curve a, the clearly distinguishable sharp peaks of the product, prepared by the soft chemical method, are indicative of high crystallinity. All of the diffraction peaks can be neatly indexed to end-centered orthorhombic ammonium aluminum hydroxide carbonate [$NH_4Al(OH)_2CO_3$] (denoted as AAHC) phase (JCPDS No. 76-1923). No other diffraction peaks were detected, indicating that no impurity exists in the AAHC:Cr^{3+} precursor. Under the assistance of PEG-20000 surfactant, the well-crystallized AAHC phase was formed during the hydrothermal treatment process. After thermal decomposition of AAHC at 1573 K, Fig. 1 curve b shows the pure α-Al_2O_3 (JPCDS No. 78-2427) phase. The diffraction peaks of Fig. 1c coincide well with the standard diffraction of AlOOH (JCPDS No.21-1307), indicating that the obtained samples are single-phase, orthorhombic AlOOH. The XRD pattern of Fig. 1d indicates that AlOOH underwent thermal transformation to α-Al_2O_3. No other phase is found, because the foreign element, such as carbon and hydrogen from the surfactant, can be oxidized easily at high temperature. Additionally, the concentration of Cr^{3+} is low, and furthermore, Cr^{3+} ions can incorporate into Al_2O_3 lattice and form substituted solid solution.

Fig. 2 shows representative SEM micrographs of the precursors and the Al_2O_3:Cr^{3+} (0.3 mol%) powders calcined at 1573 K for 2 h. As can be seen from the SEM images, the sample of Fig. 2a consists of uniformly sized microfibers with the length and diameter about 5–9 μm and 300–600 nm, respectively. The microfibers remain free-standing, remarkably with no sign of aggregation through the whole crystallization process. After thermal treatment at 1573 K, an average decrease in diameter is already noticeable. The length and diameter of the sample in Fig. 2b are about 2–5 μm and 100–300 nm, respectively. The shrinkage of the diameter is attributed to the pyrolysis of the precursor and the increase of the crystallinity. Moreover, as the calcination temperature is raised above 1573 K, the alumina microfibers synthesized in our experiment present an aggregation of the structure. The SEM micrograph depicted in Fig. 2c shows that the fibers have a very smooth surface. As shown in Fig. 3d, the sample is made up of hierarchically nanostructured microspheres with an average diameter of about 2 μm. The SEM micrograph reveals that the microspheres are built up by nanosheets. After the AlOOH:Cr^{3+} (0.3 mol%) precursor was calcined at 1573 K for 2 h. It can be found that the grains have an average diameter of 1–2 μm, and the edge angles of the grains are very smooth. What is more, there is clearly porous structure on the surface of the grains. This is

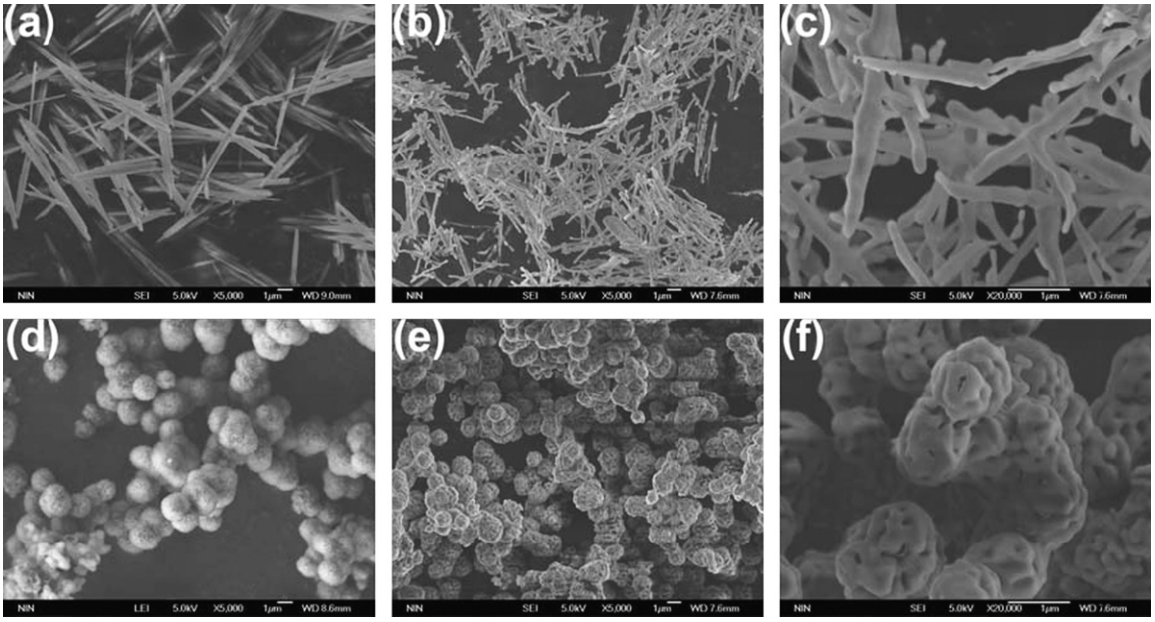

Fig. 2. SEM micrographs for precursors (a), (d) and Al_2O_3:Cr^{3+} (0.3 mol%) powders (b)–(f) prepared by methods (at 1573 K): (a)–(c) hydrothermal route, (d)–(f) microwave solvothermal method.

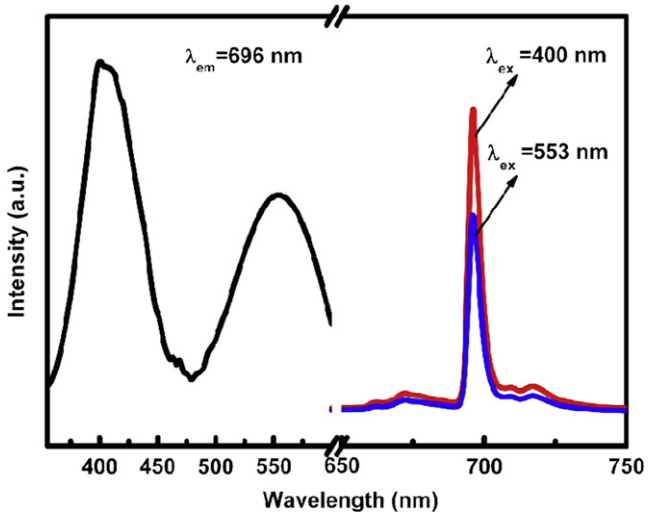

Fig. 3. Room temperature excitation (left) and emission (right) spectra for the Al_2O_3:Cr^{3+} (0.3 mol%) microfibers calcined at 1573 K, measured with a xenon lamp as a light source.

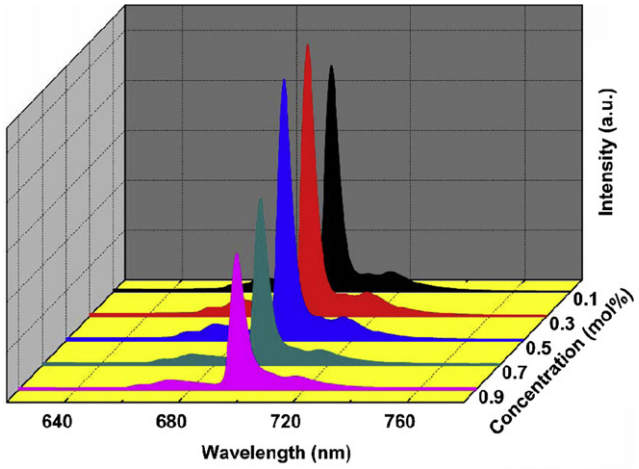

Fig. 4. Emission spectra of Al_2O_3:Cr^{3+} microfibers synthesized at 1573 K for 2 h with different doping concentrations of Cr^{3+} (0.1, 0.3, 0.5, 0. 7, 0.9 mol%).

probably induced by the completed release of H_2O and decomposition of CTAB and AlOOH processor.

3.2. Luminescence properties of Al_2O_3:Cr^{3+}

Due to the similarities in PLE and PL spectra of the samples with different Cr^{3+} concentrations, typical spectra of Al_2O_3 microfibers with 0.3 mol% Cr^{3+} content are shown in Fig. 3. As seen from the PLE spectrum monitored at 696 nm, two strong broad absorption bands with peak positions at around 400 and 553 nm, corresponding to spin-allowed $^4A_2(^4F)\rightarrow{}^4T_1(^4P)$ and $^4A_2(^4F)\rightarrow{}^4T_2(^4F)$ transitions of Cr^{3+} ions, are observed. From the PL spectrum, well-known narrow R lines at 696 nm, ascribed to the $^2E\rightarrow{}^4A_2$ transition of isolated single Cr^{3+} ions, are observed. Furthermore, the intensity is excited more with the use of 400 nm ultraviolet light than with the use of 553 nm yellow light.

Fig. 4 shows the PL spectra of Al_2O_3:Cr^{3+} microfibers synthesized at 1573 K for 2 h with different doping concentrations of Cr^{3+} (0.1, 0.3, 0.5, 0. 7, 0.9 mol%). Upon excitation at 553 nm, the red emission band at the wavelength 696 nm is from the $^2E\rightarrow{}^4A_2$ transition. The almost alike bands of PL spectra indicate that the symmetry of emitting centers of Cr^{3+} is the same. It is evident that the emission intensity strongly depends on the doping

concentration. At low Cr^{3+} concentrations ($\chi < 0.3$ mol%), the emission intensity is weak because there are not sufficient luminescence centers. However, under the condition of increasing Cr^{3+} concentration, the emission intensity increases, and reaches the maximal value at 0.3 mol%. When the Cr^{3+} doping ratio is greater than 0.3 mol%, the luminescence intensity starts to reduce as concentration quenching occurs due to the decrease in Cr–Cr distance. Based on Dexter's theory [10], the critical distance between Cr^{3+} ions for energy transfer can be calculated by the following relation:

$$R_c \approx 2\left[3V/(4\pi x_c Z)\right]^{1/3} \quad (1)$$

where V is the volume of the unit cell, x_c the critical concentration of the doping ions and Z the number of host cation in the unit cell. For α-Al_2O_3, $V=254.7$ Å^3, $Z=12$ and the critical concentration of Cr^{3+} in the α-Al_2O_3 host is 0.003. Therefore, the R_c of Cr^{3+} ions is determined to be 24 Å.

PL decay curves of Al_2O_3:Cr^{3+} microfibers with different concentrations of Cr^{3+} (0.1, 0.3, 0.5, 0.7, 0.9 mol%), shown in Fig. 5, were used to calculate the lifetime and investigate the luminescence dynamics of the samples. The samples are excited at 553 nm and monitored at 696 nm. It is found that the curves followed the single-exponential decay

$$I_t = I_0 \exp(-t/\tau) \quad (2)$$

where I_t is the intensity at time t, I_0 is the intensity at $t=0$, and τ is the decay lifetime. The fitted fluorescence lifetime values of Al_2O_3:Cr^{3+} microfibers are 4.40, 3.88, 3.24, 2.39, 2.11 ms corresponding to the Cr^{3+} concentration 0.1, 0.3, 0.5, 0.7, and 0.9 mol%, respectively.

The luminescence properties for the Al_2O_3:Cr^{3+} (0.3%) microspheres obtained by the microwave solvothermal method at 1573 K also exhibited very similar properties to those prepared by hydrothermal route at the same temperature. It can be seen in Figs. S1–S3 in the supporting information. In addition, from the comparative emission spectra of the as-obtained Al_2O_3:Cr^{3+} (0.3 mol%) microspheres and microfibers in Fig. 6, it can be seen that the two samples show similar spectral patterns without any emission band shift, but one can clearly observe that the microspheres have a higher PL intensity than the microfibers. It is well known that the surface area of materials increases along with a decrease in size. The large surface area introduces a large number of defects into the crystal, which has a serious drawback on the PL intensity of the luminescence materials. If the surface area is greatly reduced, which results from increased crystallite size, the luminescence materials with fewer defects would show great improvement in PL intensity [7,8,11]. From the SEM results presented above (Fig. 2), it can be observed that the surface area of the Al_2O_3 microspheres is lower than that of the microfibers.

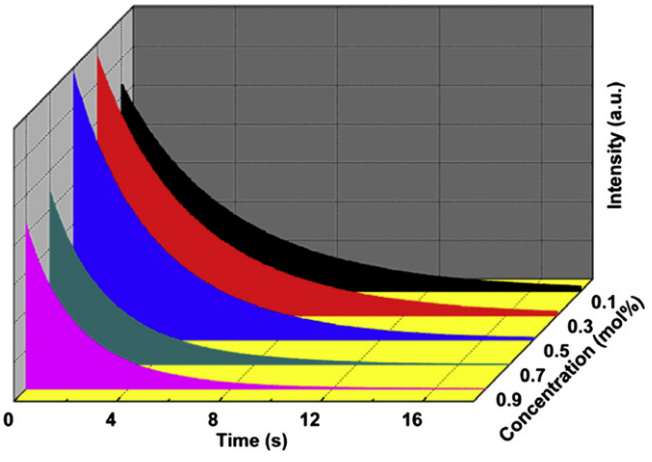

Fig. 5. The decay curves of Al_2O_3:Cr^{3+} microfibers synthesized at 1573 K for 2 h with different concentrations of Cr^{3+} (0.1, 0.3, 0.5, 0. 7, 0.9 mol%).

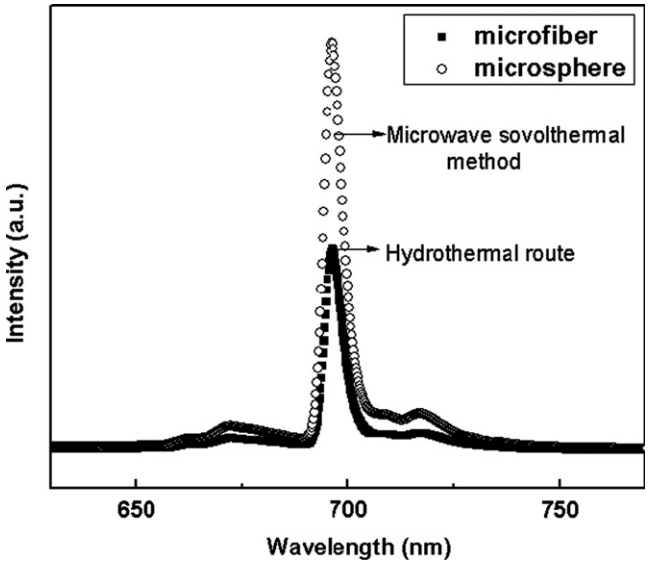

Fig. 6. Emission spectra of Al_2O_3:Cr^{3+} (0.3 mol%) microsphere and microfiber synthesized at 1573 K for 2 h.

4. Conclusions

In summary, the controllable synthesis of α-Al_2O_3:Cr^{3+} samples with different morphologies has been successfully achieved through hydrothermal and microwave solvothermal methods. The average diameter of α-Al_2O_3:Cr^{3+} microfibers was about 100–300 nm, and the length was around 2–5 μm, while the obtained α-Al_2O_3 based powders were microspheres with an average diameter about 1–2 μm. As seen from the PLE spectrum monitored at 696 nm, two strong broad absorption bands with peak positions at around 400 and 553 nm, are corresponding to spin-allowed $^4A_2(^4F) \rightarrow {}^4T_1(^4P)$ and $^4A_2(^4F) \rightarrow {}^4T_2(^4F)$ transitions of Cr^{3+} ions. From the PL spectrum, well-known narrow R lines at 696 nm, ascribed to the $^2E \rightarrow {}^4A_2$ transition of isolated single Cr^{3+} ions, are observed. From the luminescence study the optimum concentration of luminescence is found to be

0.3 mol%. The critical energy transfer distance of Cr^{3+} in Al_2O_3 host is calculated to be 24 Å. In addition, the experiment results indicate that the luminescence properties of the as-obtained luminescence materials are dependent on their doping content and morphology. As a result of the unique luminescence properties and controllable morphology, these luminescence materials may find potential applications in fields such as optoelectronic and nanoscale devices or biological technology.

Appendix A. Supplementary information

Supplementary data associated with this article can be found in the online version at http://dx.doi.org/10.1016/j.ceramint.2012.11.063.

References

[1] Y.T. Chang, H.L. Chang, K.W. Su, et al., High-efficiency Q-switched dual-wavelength emission at 1176 and 559 nm with intracavity Raman and sum-frequency generation, Optics Express 17 (2009) 11892–11897.
[2] Z.F. Zhu, D.G. Liu, H. Liu, et al., Photoluminescence properties of Tb^{3+} doped Al_2O_3 microfibers via a hydrothermal route followed by heat treatment, Ceramics International 38 (2012) 4137–4141.
[3] W.X. Wang, Z.Y. Cheng, P.P. Yang, et al., Patterning of YVO_4:Eu^{3+} luminescent films by soft lithography, Advanced Functional Materials 21 (2011) 456–463.
[4] J. Shen, L.D. Sun, J.D. Zhu, et al., Biocompatible bright YVO_4:Eu nanoparticles as versatile optical bioprobes, Advanced Functional Materials 20 (2010) 3708–3714.
[5] G.G. Li, C. Peng, C.X. Li, et al., Shape-controllable synthesis and morphology-dependent luminescence properties of GaOOH:Dy^{3+} and β-Ga_2O_3:Dy^3, Inorganic Chemistry 49 (2010) 1449–1457.
[6] G. Jia, Y.J. Huang, Y.H. Song, et al., Controllable synthesis and luminescece properties of $La(OH)_3$ and $La(OH)_3$:Tb^{3+} nanocrystals with multiform morphologies, European Journal of Inorganic Chemistry 2009 (2009) 3721–3726.
[7] J. Yang, C.X. Li, Z.Y. Cheng, et al., Size-tailored synthesis and luminescent properties of one-dimensional Gd_2O_3:Eu^{3+} nanorods and microrods, Journal of Physical Chemistry C 111 (2007) 18148–18154.
[8] B. Tang, J.C. Ge, L.H. Zhuo, The fabrication of $La(OH)_3$ nanospheres by a controllable-hydrothermal method with citric acid as a protective agent, Nanotechnology 15 (2004) 1749–1751.
[9] Y.P. Li, J.H. Zhang, X. Zhang, et al., Luminescent properties in relation to controllable phase and morphology of $LuBO_3$:Eu^{3+} nano/microcrystals synthesized by hydrothermal approach, Chemistry of Materials 21 (2009) 468–475.
[10] G. Blasse, Energy transfer in oxidic phosphors, Philips Research Reports 24 (1969) 131–144.
[11] J.X. Wan, Z.H. Wang, X.Y. Chen, et al., Shape-tailored photoluminescence intensity of red phosphor Y_2O_3:Eu^3, Journal of Crystal Growth 284 (2005) 538–543.